Development 139, 475-487 (2012) doi:10.1242/dev.067314

p57^{KIP2} regulates radial glia and intermediate precursor cell cycle dynamics and lower layer neurogenesis in developing cerebral cortex

Georges Mairet-Coello[1,*,‡], Anna Tury[1,*,§], Elise Van Buskirk[1,¶], Kelsey Robinson[2], Matthieu Genestine[1] and Emanuel DiCicco-Bloom[1,3,]**

SUMMARY

During cerebral cortex development, precise control of precursor cell cycle length and cell cycle exit is required for balanced precursor pool expansion and layer-specific neurogenesis. Here, we defined the roles of cyclin-dependent kinase inhibitor (CKI) p57^{KIP2}, an important regulator of G1 phase, using deletion mutant mice. Mutant mice displayed macroencephaly associated with cortical hyperplasia during late embryogenesis and postnatal development. Embryonically, proliferation of radial glial cells (RGC) and intermediate precursors (IPC) was increased, expanding both populations, with greater effect on IPCs. Furthermore, cell cycle re-entry was increased during early corticogenesis, whereas cell cycle exit was augmented at middle stage. Consequently, neurogenesis was reduced early, whereas it was enhanced during later development. In agreement, the timetable of early neurogenesis, indicated by birthdating analysis, was delayed. Cell cycle dynamics analyses in mutants indicated that p57^{KIP2} regulates cell cycle length in both RGCs and IPCs. By contrast, related CKI p27^{KIP1} controlled IPC proliferation exclusively. Furthermore, p57^{KIP2} deficiency markedly increased RGC and IPC divisions at E14.5, whereas p27^{KIP1} increased IPC proliferation at E16.5. Consequently, loss of p57^{KIP2} increased primarily layer 5-6 neuron production, whereas loss of p27^{KIP1} increased neurons specifically in layers 2-5. In conclusion, our observations suggest that p57^{KIP2} and p27^{KIP1} control neuronal output for distinct cortical layers by regulating different stages of precursor proliferation, and support a model in which IPCs contribute to both lower and upper layer neuron generation.

KEY WORDS: Corticogenesis, Cyclin-dependent kinase inhibitor, p27^{KIP1} (Cdkn1b), Mouse

INTRODUCTION

The mammalian cerebral cortex is organized tangentially into specific functional domains and radially into six neuronal layers. In mouse, projection neurons are generated between embryonic day 11 (E11) and E17 (Takahashi et al., 1996b) from precursors surrounding the lateral ventricles. Initially, radial glial cells (RGCs) that comprise the pseudostratified ventricular zone (VZ) divide asymmetrically at the apical surface, producing neurons for all layers (Heins et al., 2002; Malatesta et al., 2003; Anthony et al., 2004; Gotz and Barde, 2005). As neurogenesis proceeds, RGCs produce intermediate precursor cells (IPCs) that localize basally in subventricular zone (SVZ) and undergo symmetric neurogenic divisions (Haubensak et al., 2004; Miyata et al., 2004; Noctor et al., 2004). Although some studies indicate that IPCs generate upper-layer neurons exclusively (Tarabykin et al., 2001; Zimmer et al., 2004; Arnold et al., 2008; Cubelos et al., 2008), others suggest IPCs contribute to both deep and superficial layers, serving as transit-amplifying populations (Haubensak et al., 2004; Sessa et al., 2008; Kowalczyk et al., 2009).

Postmitotic neurons arising from proliferative zones migrate radially through the intermediate zone (IZ) to establish specific cortical plate layers (CP) in reverse order (Angevine and Sidman, 1961; Berry et al., 1964; Hicks and D'Amato, 1968; McConnell, 1988; Rakic, 1988; Bayer and Altman, 1991). Cells leaving the cycle early (E11-E14) generate layers 4-6, whereas those born later (E15-E17) populate layers 2-3 (Polleux et al., 1997). As the day precursors exit the cycle correlates with laminar destinations, mechanisms that regulate cycle machinery may also impact neuronal fate. G1 phase is a key point of regulation wherein precursors integrate extracellular and intracellular signals controlling cell cycle progression and withdrawal (Dehay and Kennedy, 2007). During corticogenesis, cell cycle length (T_C) increases progressively owing to elongation of G1 (T_{G1}) (Takahashi et al., 1995a). Simultaneously, the fraction of cells leaving the cycle to become neurons increases together with asymmetric and neurogenic symmetric divisions (Takahashi et al., 1996b). Recent studies suggest a link between T_{G1}, precursor pool size and neurogenesis. Deletion of cyclin D2 lengthens T_{G1}, eliciting premature cycle withdrawal, precursor depletion and reduced neurogenesis (Glickstein et al., 2009). Conversely, D cyclin overexpression reduces cycle length and promotes RGC and IPC cycle re-entry, expanding precursors pools and superficial layer neurogenesis (Lange et al., 2009; Pilaz et al., 2009).

Cyclin-dependent kinase inhibitors (CKIs) of the CIP/KIP family, including p57^{KIP2} (*Cdkn1c* – Mouse Genome Informatics) and p27^{KIP1} (*Cdkn1b* – Mouse Genome Informatics), regulate G1/S

[1]Department of Neuroscience and Cell Biology, UMDNJ-Robert Wood Johnson Medical School, Piscataway, NJ 08554, USA. [2]Rutgers University, Piscataway, NJ 08554, USA. [3]Department of Pediatrics, UMDNJ-Robert Wood Johnson Medical School, New Brunswick, NJ 08903, USA.

*These authors contributed equally to this work
‡Present address: The Scripps Research Institute, Dorris Neuroscience Center, La Jolla, CA 92037, USA
§Present address: University of California, San Diego, Division of Biological Sciences, La Jolla, CA 92093, USA
¶Present address: Department of Biology, Duke University, Durham, NC 27708, USA
**Author for correspondence (diciccem@umdnj.edu)

Accepted 22 November 2011

transition by inhibiting cyclin/CDK complexes (Sherr and Roberts, 1999). Moreover, CKIs also regulate many aspects of neurogenesis, including developmental roles for $p57^{KIP2}$ in dopamine-containing (Joseph et al., 2003) and retinal amacrine neurons (Dyer and Cepko, 2000), and effects of $p27^{KIP1}$ on neuron differentiation and migration (Nguyen et al., 2006; Itoh et al., 2007). Our evidence that CKIs differentially regulate neuroglial fate depending on environmental signals and developmental stage (Tury et al., 2011). Given their functions during G1, CKIs are positioned to control cell cycle dynamics, including T_{G1}, precursor pool size and neuronal output. Although $p27^{KIP1}$ regulates cell cycle re-entry and upper layer neurogenesis, but surprisingly not T_{G1} (Delalle et al., 1999; Goto et al., 2004; Tarui et al., 2005; Suter et al., 2007; Caviness et al., 2008), $p57^{KIP2}$ roles are undefined. Significantly, $p57^{KIP2}$ is more abundantly expressed during early corticogenesis (Tury et al., 2011), raising the question of whether CKIs differentially regulate precursor proliferation and laminar neurogenesis. We demonstrate that $p57^{KIP2}$ regulates cell cycle dynamics of RGCs and IPCs, with greater impact on IPCs, and controls precursor pool size, neuron production, cortical size and laminar patterning. Furthermore, $p57^{KIP2}$ regulates both RGC and IPC proliferation, and layer 5-6 neurogenesis, whereas $p27^{KIP1}$ controls IPCs and layer 2-5 neurogenesis exclusively.

MATERIALS AND METHODS

Animals

$p57^{KIP2+/-}$ mice were from Stephen Elledge (Zhang et al., 1997). As the $p57^{KIP2}$ gene is imprinted, i.e. expressed from maternal but not paternal allele, mutants heterozygous for defective maternal allele ($p57^{KIP2+/m-}$) exhibit the same phenotype as nulls ($p57^{KIP2-/-}$). Absence of $p57^{KIP2}$ expression in $p57^{KIP2+/m-}$ embryo cortex was verified by RT-PCR (supplementary material Fig. S1). In addition, western blotting, real-time PCR studies and observations from immunohistochemistry revealed no difference in $p27^{KIP1}$ protein levels/localization or gene expression in $p57^{KIP2+/m-}$ cortices (data not shown). $p27^{KIP1+/-}$ mice were obtained from Jackson Laboratory (Fero et al., 1996). Both lines were maintained on C57BL/6 background. Experiments were performed on wild-type, $p57^{KIP2+/m-}$ (p57KO) and $p27^{KIP1}$-null mutants (p27KO).

The day of plug was considered to be E0.5 and day of birth to be postnatal day 0 (P0). All procedures conformed to IACUC and NIH guidelines.

Dissociated cell culture and S-phase entry

Cortical cells (1750 cells/mm^2) from E15.5 embryos were plated on poly-D-lysine (5 μg/ml, Sigma)-coated dishes, in defined medium composed of DMEM/F12-containing penicillin (50 U/ml), streptomycin (50 μg/ml), transferrin (100 μg/ml), putrescine (100 μM), progesterone (20 nM), selenium (30 nM), glutamine (2 mM), glucose (6 mg/ml) and BSA (10 mg/ml) (Mairet-Coello et al., 2009). Cultures were incubated at 37°C with 5% CO_2.m

The BrdU labeling index was determined following a 2-hour BrdU pulse, counting 4000-7000 cells/dish from 10 random fields in three dishes/group (Mairet-Coello et al., 2009).

DNA quantification

Brains from E17.5 embryos were dissected from rostral-to-occipital end (excluding olfactory bulbs). DNA was quantified using DNA dye-binding assay (Mairet-Coello et al., 2009). DNA was extracted from homogenates by 10% trichloroacetic acid (TCA) precipitation. Pellet was treated with 1 N KOH and sedimented using 5% TCA. After solubilization (90°C), supernatants of samples and standards (calf thymus DNA) were incubated with diphenylamine reagent at 37°C overnight and optical densities measured at 600 nm.

[^{3}H]Thymidine incorporation

[^{3}H]Thymidine incorporation was used as a marker of DNA synthesis (Mairet-Coello et al., 2009). Cultures were incubated with 1 μCi/ml [^{3}H]thymidine (Amersham) for 2 hours before termination, and incorporation determined by scintillation spectroscopy. For in vivo studies, tissues were homogenized in distilled water and equal volumes were used to determine total isotope in the tissue and incorporated into DNA. DNA was precipitated with 10% TCA. Pellet and original homogenate were dissolved and processed for scintillation spectroscopy. Percentage incorporation is the ratio of radiolabel incorporated into DNA to total tissue uptake.

Western blotting

Tissue homogenization and western blotting were conducted as described (Mairet-Coello et al., 2009). The pooled right and left cortices were homogenized in lysis buffer containing 50 mM Tris HCl (pH 7.5), 150 mM NaCl, 10 mM EDTA, 2 mM EGTA, 1% CHAPS, 0.5% NP-40, 1% Triton X100 and protease inhibitors. Following sonication, lysates were centrifuged at 20,000 ***g*** for 20 minutes. Supernatants were assayed for protein using Bio-Rad Assay (Bio-Rad).

Proteins were separated by SDS-PAGE and transferred to PVDF membranes. Membranes were blocked with 5% fat-free dry milk in Tris-buffered saline containing 0.05% Tween20 and incubated overnight (4°C) with the following primary antibodies: Cux1 (1:200, Cell Signaling); Tbr1 (1:1000, Chemicon); β-actin (1:5000, Chemicon); cleaved-caspase-3 (1:1000, Cell Signaling).

To assess loading, blots were stripped and reanalyzed for β-actin. Autoradiographic film signals were quantified using Bio-Rad Gel Doc 2000 with Quantity One.

Immunohistochemistry

Brain sections were processed for immunofluorescence or immunoperoxidase (Mairet-Coello et al., 2005). Sections (12 μm) were obtained using a cryostat (Leica) and submitted to antigen retrieval by steam in 10 mM citrate buffer (pH 6), at 90-95°C for 5-15 minutes (Tang et al., 2007). Primary antibodies, diluted in PBS containing 0.3% Triton X-100, 10% lactoproteins and 1% BSA, were incubated overnight. Primary antibodies included: $p57^{KIP2}$ (1:40, sc-8298/H-91, Santa-Cruz); $p27^{KIP1}$ (1:1000, BD-Pharmingen); bromodeoxyuridine (BrdU) (1:100, mouse, Becton-Dickinson Biosciences; 1:100, rat, AbD Serotec); iododeoxyuridine (IdU)/BrdU (1:200, Invitrogen); phospho-histone H3 (1:200, Upstate); Ki67 (1:500, Novocastra); PCNA (1:2000, Santa-Cruz); Pax6 (1:500, rabbit, Chemicon); Pax6 (1:100, mouse, 1-223, developed by Dr. A. Kawakami, Tokyo Institute of Technology, Yokohama, Japan, and obtained from the Developmental Studies Hybridoma Bank); Tbr2 (1:500, Chemicon); bIII-tubulin/TuJ1 (1:1000, Covance); Tbr1 (1:1000); Ctip2 (1:400, Santa Cruz); Cux1 (1:200, Santa Cruz); cleaved-caspase-3 (1:200); parvalbumin (1:1000, SWANT); S100β (1:1000, Sigma); CC1 (1:200, Calbiochem); NeuN (1:1000, Chemicon). Labeling was visualized using Alexa Fluor secondary antibodies (Invitrogen) and sections were counterstained with propidium iodide or DAPI. Immunoperoxidase staining was visualized using 3,3′-diaminobenzidine and sections counterstained with Toluidine Blue. For double immunolabeling using $p57^{KIP2}$ and Tbr2 antibodies, both of which were derived from rabbit, sections were labeled for $p57^{KIP2}$ by immunoperoxidase followed by Tbr2 immunofluorescence, using published protocols (Mairet-Coello et al., 2005). Images of $p57^{KIP2}$ staining were inverted, pseudocolored and merged with Tbr2 immunofluorescence.

Image acquisition and analyses

Cultures and tissue sections were examined with bright-field (Axiophot) or fluorescence microscopes (Axiovert 200M, Carl Zeiss). The fluorescent microscope was equipped with NeoFluar objectives and coupled to Apotome under AxioVision control. Large images were reconstructed by merging 40× objective acquisitions using Photomerge (Adobe Photoshop). Counting and morphometry were performed using Image Pro Plus (Media Cybernetics), based on established boundary criteria (Alvarez-Bolado and Swanson, 1996).

Cell cycle dynamics

Analyses in vivo were performed at mid-hemisphere in presumptive somatosensory area, including left and right dorsomedial cortices of 3-6 non-consecutive frontal (coronal) sections/brain.

RGCs and IPCs distinction

The embryonic VZ is mainly populated by Pax6+/Tbr2– RGCs, but also contains increasing numbers of Tbr2+/Pax6– IPCs and a minority of double-labeled cells transitioning from RGC to IPC. The SVZ is essentially constituted of Tbr2+/Pax6– IPCs (Englund et al., 2005; Kowalczyk et al., 2009). Since distinguishing RGCs from IPCs in the VZ requires double Pax6/Tbr2 labeling, which we did not perform, our cell cycle analyses may reflect a mixed precursor population.

BrdU labeling index

BrdU (50 μg/g body weight) was injected intraperitoneally into pregnant dams 30 minutes or 2 hours before sacrifice. The labeling index was determined by counting BrdU+ cells over total cells (~2000 cells/animal) within 100 μm bins extending from ventricular surface to VZ/SVZ boundary, defined as the upper limit of dense, BrdU+ cells (Takahashi et al., 1993).

Apical and basal mitoses

Mean numbers of mitoses/cortical area were estimated by counting phospho-histone H3 (PH3)-labeled nuclei on frontal sections. Localization to apical (VZ) or basal (SVZ) regions allowed assignment to RGC or IPC populations, respectively (Sessa et al., 2008).

Growth fraction in the VZ

The growth fraction, defined as the proportion of proliferating cells, was assessed using cumulative BrdU injections into E14.5 pregnant females every 3 hours (Takahashi et al., 1995a). It corresponds to the maximal achievable BrdU labeling index in the VZ. Alternatively, numbers of Ki67+ cells over total cells (DAPI) were determined in VZ of E12.5, E14.5 and E16.5 wild-type and p57KO embryos. Values were similar in both genotypes and approached 100% (not shown).

Cell cycle length of VZ precursors

Cell cycle length was measured using IdU and BrdU markers, based on published methods (Hayes and Nowakowski, 2000; Martynoga et al., 2005; Quinn et al., 2007). Pregnant dams first received intraperitoneal injection of IdU followed by BrdU at 1.5 hours (both at 70 μg/g body weight) and were sacrificed at 2 hours. Cortical frontal sections were double immunolabeled for IdU/BrdU and stained with DAPI for total cells. Lengths of S phase (T_S) and total cell cycle (T_C) were calculated as described previously (Martynoga et al., 2005): $T_S=1.5\times S_{cells}/L_{cells}$ and $T_C=T_S\times P_{cells}/S_{cells}$ [L_{cells}=leaving fraction cells (identified as IdU+ and BrdU–); S_{cells}=cells in S phase (identified as double BrdU+/IdU+); P_{cells}=total proliferating cells (labeled with DAPI)]. Combined length of G2 and M (T_{G2+M}) was estimated following a 2-hour BrdU pulse (Takahashi et al., 1995a). Percentage of mitotic figures (PH3+) labeled with BrdU was identical in wild-type and p57KO embryos (6 sections/animal), with ~100% of mitotic figures BrdU co-labeled. Therefore, T_{G2+M}=~2 hours. Finally, $T_{G1}=T_C-(T_S+T_{G2+M})$.

Relative cell cycle length in SVZ

To assess relative changes in IPC cycle length, we measured SVZ BrdU labeling index using BrdU/Ki67 dual immunolabeling (Arnold et al., 2008). Embryos were collected 2 hours after BrdU injection into pregnant dams and sections were immunolabeled. Ki67 was used to identify proliferating precursors in SVZ. The VZ, characterized by elliptical vertically oriented nuclei with DAPI staining (Takahashi et al., 1995b), was excluded from the assessment.

Proliferative (cell cycle re-entry) and quiescent (cell cycle exit) fractions

The balance between cell cycle re-entry and exit was determined using BrdU/Ki67 immunolabeling (Chenn and Walsh, 2002). Embryonic brains were collected 24 hours after BrdU injection into pregnant dams. Sections were immunolabeled and counterstained with DAPI. Cells that re-entered the cycle at 24 hours were BrdU+/Ki67+ (Np), while those that exited were BrdU+/Ki67– (Nq). The total number of BrdU+ cells (Np+Nq) was counted within a bin based on the ventricular surface and extending to the pia. The percentage of cells re-entering the cycle equals Np/(Np+Nq) and those leaving equals Nq/(Np+Nq). The distribution of Nq cells was analyzed on the same sections using previously described methods (Takahashi et al., 1996a; Goto et al., 2004). The cortical wall was divided into bins 150 μm wide and 10 μm high from ventricle to the lower limit of the CP and Nq cells were counted in each bin.

Unbiased stereology

Total cell numbers in the entire E18.5 cortex or specific cortical layers were counted on a series of frontal sections stained with Toluidine Blue or for layer-specific markers using the appropriate primary antibody by unbiased stereology (Vaccarino et al., 1999), using the optical dissector (Bioquant Image Analysis System).

Mean numbers of Pax6+ and Tbr2+ precursors/section in the left plus right cortex was estimated at E16.5 by stereology from three non-consecutive frontal sections at mid-hemisphere. Technical limitations of immunoperoxidase did not allow assessment of double labeled Pax6+/Tbr2+ precursors. The same method was applied at P10 to determine glial cells and interneurons using S100β and parvalbumin.

Mean cellular densities in marginal zone (MZ), CP, IZ and VZ/SVZ of E18.5 embryos were determined by counting cells/dissector in each area on four non-consecutive sections at mid-hemisphere.

Morphometry

Whole cortical volumes were estimated from a series of Toluidine Blue stained E18.5 frontal sections using Cavalieri's principle (Vaccarino et al., 1999).

Cortical extension measurements were performed on E18.5 frontal and sagittal sections (four sections/animal) using Image Pro Plus. Anterior-posterior extension was measured at the pial surface on sagittal sections, from olfactory bulb/frontal cortex boundary to occipital cortex/dorsal subiculum boundary. Mean cortical thickness was measured throughout the rostrocaudal extent on the same sagittal sections. Medial-lateral extension was measured at the pial surface on frontal sections at mid-hemisphere, from ventral retrosplenial area to rhinal fissure.

CP and laminar thicknesses were assessed on E18.5 sagittal sections labeled with Tbr1 and Cux1. Thicknesses were measured at four anteroposterior positions separated by 700 μm in mediodorsal and lateral cortices.

Birthdating analyses

Pregnant mice were injected with BrdU at E13.5 and sacrificed at E19.5. Frontal sections were triple immunolabeled for BrdU, Ctip2 and Tbr1. The distribution and types of neurons born on E13.5 were analyzed in dorsomedial cortex at mid-hemisphere using established methods (Molyneaux et al., 2005). CP was divided into nine or three bins of equal height and fixed width. Cells with strong, homogenous nuclear BrdU labeling, corresponding to neurons born on E13.5, were counted in each bin. The proportions of BrdU+ cells expressing Tbr1 or Ctip2 over the total number of BrdU+ cells was determined in each bin.

Data analysis and statistics

Statistical analyses were performed using Student's *t* (two-tailed) test in GraphPad InStat (GraphPad). All data are expressed as means or percents±s.e.m. *$P<0.05$, **$P<0.01$, ***$P<0.001$.

RESULTS

p57KO embryos exhibit macroencephaly

To address p57KIP2 roles in cortical development, we examined p57KO mice. Because mutants die perinatally from cleft palate and respiratory difficulty (Zhang et al., 1997), observations were conducted in embryos, though rare survivors were examined at P10. Mutant brains at E18.5 are morphologically normal, but larger, especially cerebral cortex and midbrain (Fig. 1A-C). Brain weight was increased during late embryogenesis, together with body weight (Fig. 1D; supplementary material Fig. S1B). DNA content, a marker for total cells, was increased, suggesting increased cell production (Fig. 1E).

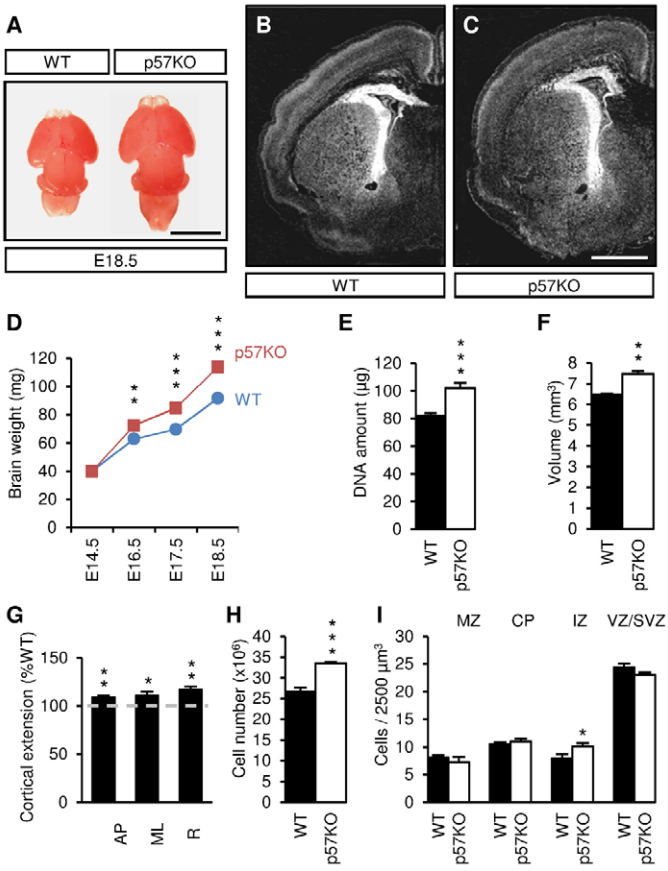

Fig. 1. p57KO embryos exhibited brain enlargement. (**A-C**) p57KO brains exhibited larger cerebral cortex and midbrain. (**D**) p57KO brain weights were increased during late embryogenesis (*n*=16-35/group). (**E**) DNA content was increased in E17.5 mutant brains (*n*=8-9/group). (**F**,**G**) Volumes of E18.5 p57KO cortices were increased by 15% (F) due to augmented anterior-posterior (AP), mediolateral (ML) and radial (R) lengths (G). Values expressed as percent control (*n*=4/group). (**H**,**I**) Total cell number was increased by 23% in E18.5 p57KO cortices (H), with cell density increased only in IZ (*n*=4/group) (I). Data are mean±s.e.m. **P*<0.05, ***P*<0.01, ****P*<0.001. Scale bars: 5 mm in A; 1 mm in B,C.

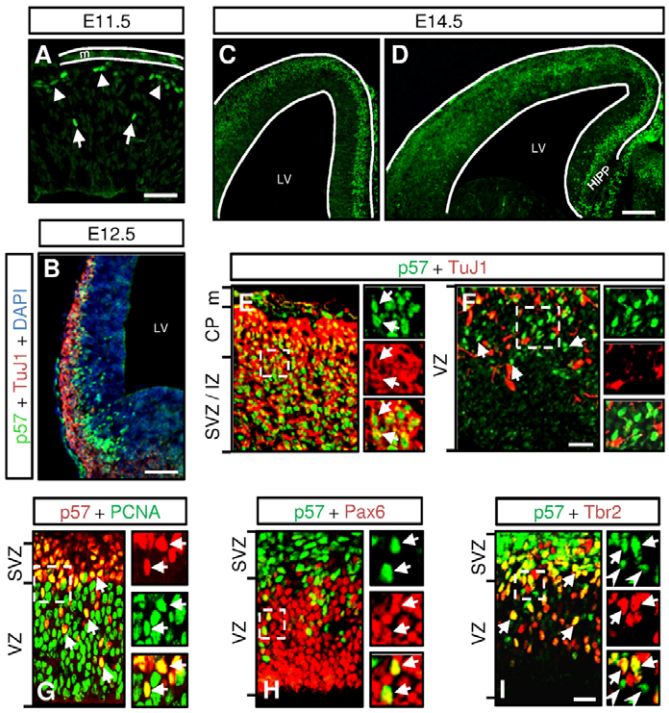

Fig. 2. p57^{KIP2} protein expression in proliferating precursors and postmitotic neurons during development. (**A**) p57^{KIP2} was detected at E11.5 in cells in peripheral cortex (arrowheads) with few cells in the proliferative zone (arrows). (**B**) At E12.5, p57^{KIP2} localized to a dense group of cells laterally, including precursors (TuJ1–) and newborn neurons (TuJ1^{+}). (**C-I**) At E14.5, p57^{KIP2+} cells increased considerably in isocortex and hippocampus (HIPP), detected on anterior (C) and mid-hemisphere (D) sections. p57^{KIP2} was present (E) in TuJ1^{+} postmitotic neurons (arrows, insets) and in (F) TuJ1^{-} cells in proliferative zones (arrows). (**G**) p57^{KIP2} was expressed in PCNA^{+} proliferating cells (arrows) and in (H) Pax6^{+} and (I) Tbr2^{+} cells (arrows). Arrowheads in I indicate p57^{KIP2+}/Tbr2^{-} cells. Scale bars: 25 µm in G-I; 50 µm in A,E,F; 100 µm in B; 200 µm in C,D.

Overall cortical volume was increased at E18.5 (Fig. 1F), with increased anterior-posterior, medial-lateral and radial dimensions (Fig. 1G) as well as dorsomedial cortical wall thickness (supplementary material Fig. S2). Total cell number in mutant cortex was increased by 23%, whereas cell density was only increased in the IZ (Fig. 1H,I). Collectively, these observations indicate that cortical surface, thickness and cell number are increased during late embryonic development in the absence of p57^{KIP2}.

p57^{KIP2} is expressed in Pax6^{+} and Tbr2^{+} precursors, and postmitotic neurons

Previous studies in cortex report either divergent patterns or absent p57^{KIP2} protein expression (Nguyen et al., 2006; Itoh et al., 2007; Glickstein et al., 2009). Although we recently defined p57^{KIP2} expression in E14.5 mouse using a well-characterized antibody (Tury et al., 2011), we now fully characterize developmental expression. p57^{KIP2} was detected at the onset of neurogenesis E11.5 (Fig. 2A), present in cell nuclei at the periphery, with few cells in proliferative regions. At E12.5, numerous labeled cells were observed in lateral cortex with few medially, a pattern roughly following the lateromedial gradient of neurogenesis, and reflected by differentiation marker TuJ1 (Fig. 2B). At E14.5, p57^{KIP2}-labeled cells increased considerably, localizing mainly to cell nuclei of CP and IZ, and proliferative regions (Fig. 2C-F). Besides cortex, p57^{KIP2} immunoreactivity was observed in hippocampus (Fig. 2D). At cellular levels, p57^{KIP2} colocalized with DAPI in nuclei in proliferative and postmitotic compartments (data not shown).

To characterize cells expressing p57^{KIP2}, we performed double immunolabeling. At E14.5, the cortex comprises two postmitotic compartments (IZ and CP), and two proliferative regions: (1) the VZ, containing mainly Pax6^{+}/Tbr2^{-} RGCs, some Tbr2^{+}/Pax6^{-} IPCs, and few Pax6^{+}/Tbr2^{+} IPCs transitioning from RGCs; and (2) SVZ, mainly containing Tbr2^{+}/Pax6^{-} IPCs (Englund et al., 2005; Kowalczyk et al., 2009). p57^{KIP2} was expressed primarily in TuJ1^{+} postmitotic neurons in CP and IZ (Fig. 2E), but also TuJ1^{-} cells in VZ and SVZ (Fig. 2F). Furthermore, 36.6±1.3% of total p57^{KIP2+} cells co-localized PCNA, with 62.8±3.4% in the VZ and 41.4±2.4% in SVZ (Fig. 2G). To label RGC and IPC precursors,

we used Pax6 or Tbr2: 11.1±0.6% of Pax6$^+$ cells expressed p57^{KIP2} whereas 45.3±0.6% of Tbr2$^+$ cells co-labeled (Fig. 2H,I). Owing to technical limitations, we were unable to triple label p57^{KIP2}, Pax6 and Tbr2 to confirm p57^{KIP2} expression in Pax6$^+$/Tbr2$^-$ RGCs. Altogether, these results suggest p57^{KIP2} may regulate cell cycle dynamics in IPCs, and potentially in RGCs.

In the absence of p57^{KIP2}, increased cortical precursors enter S phase in cell-autonomous fashion

Increased cortex cell numbers in mutants suggest enhanced precursor proliferation. In agreement, DNA synthesis was increased in E16.5 p57KO forebrain, including cortex, hippocampus, basal ganglia and diencephalon (Fig. 3A). This did not reflect enhanced survival as there was no difference in activated caspase 3 protein levels (Fig. 3B) or immunoreactive cell numbers (wild type, 3.3±0.88; p57KO, 3.6±0.88 cells/frontal section; *n*=3 embryos/group, four sections/animal). Rather, S-phase entry, assessed by BrdU immunolabeling after a 30-minute pulse, was increased in p57KO VZ at E16.5 (but not E14.5, Fig. 3D). When we increased the S-phase-labeled cohort, using a 2-hour BrdU pulse, we detected an increased labeling index in mutants at both ages (Fig. 3D). However, results at 2 hours may reflect increased S-phase entry with a minor contribution of precursor mitosis. Isolated cortical cells from E15.5 mutants exhibited twofold increases in both DNA synthesis and the BrdU labeling index in culture, indicating that enhanced S-phase entry occurs in cell-autonomous fashion (Fig. 3C). Collectively, these observations suggest that in the absence of p57^{KIP2}, mitotic precursors are increased by changes in cell cycle dynamics rather than cell survival.

Finally, aberrant cell cycle re-entry of postmitotic cells in p57KO CP was not seen using proliferation markers PCNA, BrdU and PH3 (not shown), indicating p57^{KIP2} is not required to maintain neurons in a postmitotic state or that compensatory mechanisms intervene.

Proliferation of RGCs and IPCs is increased in p57KO mice, expanding both precursor pools

As p57^{KIP2} is expressed in cortical precursors, we wondered whether RGC and IPC proliferation changed in its absence. We quantified proliferation by counting apical (RGC) and basal (IPC) precursor divisions (PH3$^+$) at specific developmental times: E12.5 (peak layer 6 neurogenesis), E14.5 (peak layers 4-5 neurogenesis), E16.5 (peak layers 2-3 neurogenesis) and E18.5 (end of corticogenesis). Because brain size was altered in p57KO, we analyzed PH3$^+$ cells/cortical layer area (Fig. 4A-D) and per cortical section (supplementary material Fig. S3A-C). Both analyses yielded similar profiles. There was no difference in cell divisions at E12.5 (supplementary material Fig. S3A-C), suggesting p57^{KIP2} plays little role in cycle control during early corticogenesis, consistent with its sparse expression (Fig. 2A,B) and implying that increased cell numbers at E18.5 (Fig. 1H) does not result from increased founder cells. The most profound impact of p57^{KIP2} deletion occurred at E14.5 (Fig. 4A-D), with a greater increase in basal divisions (+90.6%) and a more modest change in apical divisions (+18.8%), indicating p57^{KIP2} regulates cell cycle dynamics in both RGCs and IPCs. Cell divisions decreased in both genotypes as neurogenesis proceeded (Fig. 4A; supplementary material Fig. S3A-C), suggesting p57^{KIP2} does not regulate its termination, though a modest increase in basal divisions/section (supplementary material Fig. S3C) raised the possibility that proliferation extended beyond the normal period. Differences in the

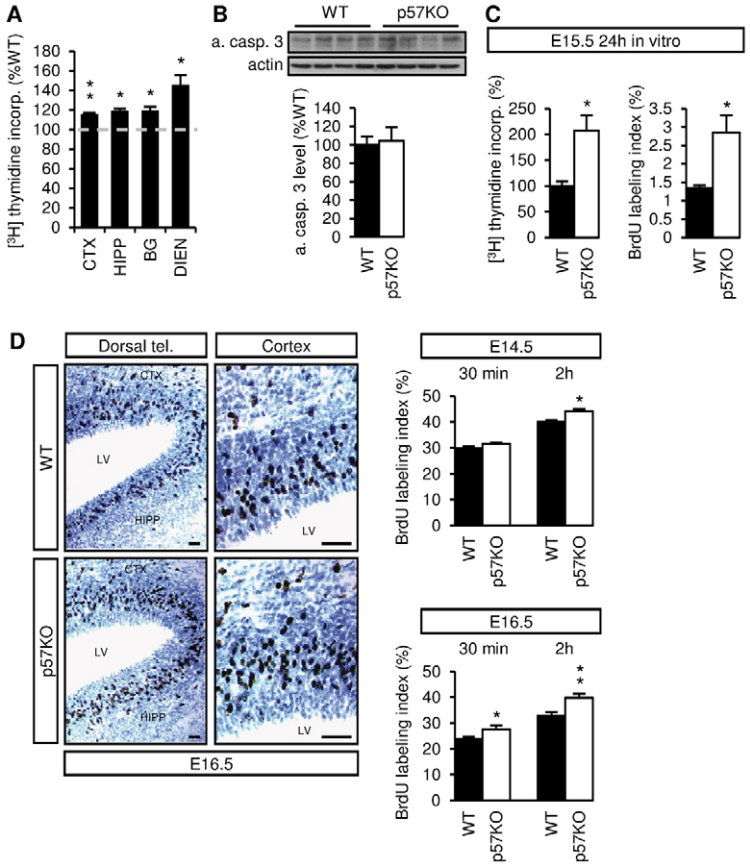

Fig. 3. p57KO cortical precursors exhibited increased DNA synthesis and S-phase entry in vivo and in vitro in cell-autonomous fashion. (**A**) DNA synthesis, measured as percentage of [^{3}H]thymidine incorporation, was increased in cerebral cortex (CTX), hippocampus (HIPP), basal ganglia (BG) and diencephalon (DIEN) of p57KO embryos at E16.5. Values represent percentage change compared with control (*n*=5-6 embryos/group). (**B**) Activated caspase 3 protein levels (a. casp. 3; 17 and 19 kDa) did not differ at E16.5 by western blot (*n*=4/group). (**C**) [^{3}H]Thymidine and BrdU were added to E15.5 cortical cultures 2 hours before termination. DNA synthesis (*n*=7-13/group) and BrdU labeling index (*n*=3/group) were increased twofold 24 hours in p57KO precursors. (**D**) BrdU was injected into pregnant dams 30 minutes or 2 hours before sacrifice. LV, lateral ventricle. Scale bars: 50 μm. BrdU$^+$ and total cells were counted in dorsomedial VZ at mid-hemisphere on frontal sections. BrdU labeling index was increased in p57KO cortex at E14.5 and E16.5 with greater effect following a 2-hour pulse (*n*=3-6/group). Data are mean±s.e.m. **P*<0.05, ***P*<0.01.

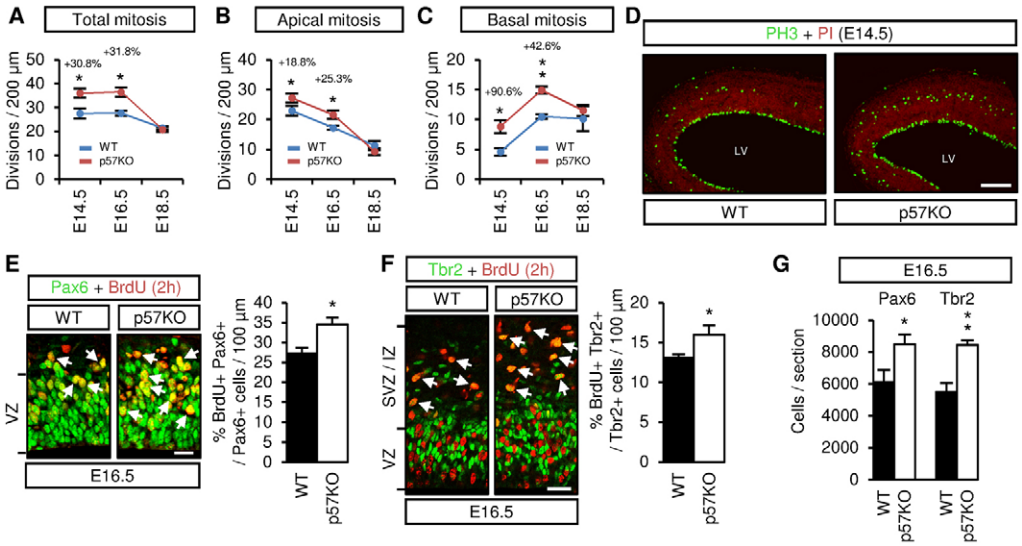

Fig. 4. Both RGC and IPC proliferation were increased in p57KO cortex producing tangential precursor pool expansion. (**A-C**) Quantification of (A) total, (B) apical and (C) basal PH3$^+$ cells/area within a 200 µm wide bin in dorsomedial cortex at mid-hemisphere from E14.5 to E18.5 (*n*=4-5 embryos/genotype/age). (**D**) E14.5 frontal sections labeled for PH3. LV, lateral ventricle. (**E**,**F**) E16.5 frontal sections were double-stained for (E) Pax6 or (F) Tbr2 and BrdU following a 2-hour pulse. Arrows indicate double labeling. Both Pax6$^+$/BrdU$^+$ and Tbr2$^+$/BrdU$^+$ cells were increased by over 20% in dorsomedial cortex in p57KOs (*n*=4-7 animals/group). (**G**) At E16.5, numbers of Pax6$^+$ and Tbr2$^+$ precursors per entire cortical section, assessed by stereology, were increased in p57KO (*n*=4/group). Data are mean±s.e.m. *P<0.05, **P<0.01. Scale bar: 200 µm in D; 25 µm in E,F.

numbers of divisions/area (Fig. 4A-D) versus divisions/section (supplementary material Fig. S3A-C) suggest gradients of neurogenesis along the mediolateral axes.

Furthermore, we determined proportions of Pax6$^+$ and Tbr2$^+$ precursors engaged in S phase following a 2-hour BrdU pulse. At E16.5, Pax6$^+$ cells in S phase localized to the VZ, while Tbr2$^+$/BrdU$^+$ cells were primarily in IZ and SVZ (Fig. 4E,F). Pax6$^+$ and Tbr2$^+$ precursors in S phase were both increased by 20% in mutants.

The foregoing analyses predict expansion of both apical and basal precursor pools. Although there were no changes in Pax6$^+$ and Tbr2$^+$ cells/area (within a radial column) at E13.5, E14.5 and E16.5 (data not shown), total numbers of Pax6$^+$ and Tbr2$^+$ cells, defined stereologically on frontal sections, increased by 39% and 54%, respectively, at E16.5 (Fig. 4G). Thus, both apical and basal precursor pools are expanded in p57KO mice, and precursors undergo tangential dispersion (parallel to the ventricle surface), rather than accumulating radially.

Cell cycle length of basal and apical precursors is shortened during middle and late corticogenesis in p57KO embryos

As proliferation was increased in the absence of p57^{KIP2}, we examined cell cycle dynamics by measuring cycle phase lengths in the VZ. At E12.5, there were no differences in phase lengths between genotypes (Table 1), consistent with unaltered proliferation. At E14.5 and E16.5, when p57^{KIP2} expression is abundant and proliferation is increased in mutants, there were marked reductions in total cell cycle times in p57KOs, by 21% and 27%, respectively. This was caused by shortening of G1 phase, and potentially a small but non-significant decrease in S phase (Table 1). Furthermore, there were no differences in proliferating VZ cells (growth fraction; see Materials and methods; cumulative BrdU labeling at E14.5: wild type, 90.1±0.01%; p57KO, 89.0±0.01%; P>0.05), supporting the contention that measurements were not biased by potential migration defects.

To assess relative changes in SVZ cell cycle dynamics, we measured BrdU labeling index (2-hour pulse) in SVZ precursors (Ki67$^+$) at E14.5, when increased basal divisions have peaked in mutants (Fig. 4C; supplementary material Fig. S3C). There were no differences in numbers of proliferating Ki67$^+$ cells/area in mutant SVZ (Fig. 5A), supporting our observations that precursors undergo tangential (but not radial) expansion. However, there was a twofold increase in both precursors engaged in S phase (BrdU$^+$/Ki67$^+$ cells; Fig. 5A) and mitotic divisions (PH3$^+$; Fig. 5B) in mutants, suggesting p57KO SVZ precursors have a faster cell cycle. These observations suggest p57^{KIP2} is a major regulator of cell cycle kinetics in both RGCs and IPCs.

Table 1. Cell cycle phase durations (hour) of VZ precursors in wild-type and p57KO embryos

Age	Genotype	T_{G1}	T_S	T_{G2+M}	T_C	% T_C change
E12.5	Wild type	3.81±0.30	4.74±0.42	2.31±0.16	10.85±0.68	
	p57KO	4.55±0.31	3.65±0.31	2.28±0.14	10.47±0.36	–3.5%
E14.5	Wild type	8.71±0.29	4.83±0.34	2.08±0.03	15.63±0.52	
	p57KO	6.31±0.49**	3.91±0.25	2.11±0.07	12.34±0.80*	–21.1%
E16.5	Wild type T	11.11±0.94	4.12±0.18	2.13±0.05	17.35±1.14	
	p57KO	6.99±0.49**	3.48±0.31	2.11±0.05	12.58±0.70**	–27.5%

Data are mean±s.e.m.*P<0.05, **P<0.01.

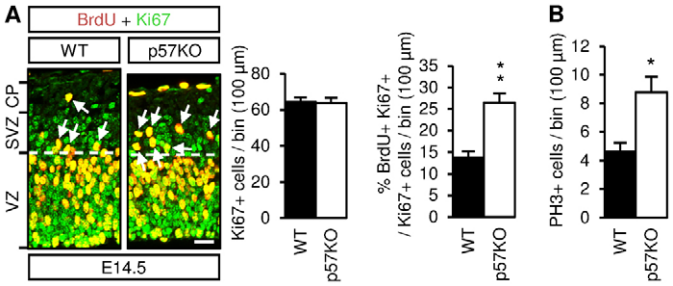

Fig. 5. Cell cycle length of SVZ precursors was shorter in p57KO. (**A**) E14.5, wild-type and p57KO cortices (frontal sections) were double labeled for Ki67 and BrdU following a 2-hour pulse. Arrows indicate double-labeled cells in SVZ. There was no difference in proliferating precursors (Ki67$^+$)/bin in SVZ between genotypes. However, SVZ precursors in S phase (Ki67$^+$/BrdU$^+$/bin) as well as mitoses (**B**) (PH3$^+$/bin) were increased twofold in mutant cortex, suggesting a reduced cell cycle length (n=3 animals/group). Data are mean±s.e.m. *P<0.05, **P<0.01. Scale bar: 25 µm.

Cell cycle re-entry is increased early while cell cycle exit is increased during later corticogenesis

To define the effects of p57^{KIP2} on the balance between proliferation and differentiation, we assessed cell cycle exit/re-entry 24 hours after a BrdU pulse. Cells remaining in cycle are BrdU$^+$/Ki67$^+$, while cells that exited exhibit BrdU labeling only (Chenn and Walsh, 2002). At E13.5, 32% fewer cells left the cycle in p57KO mutants (Fig. 6A), a change accompanied by 25% fewer TuJ1$^+$ neurons (Fig. 6B), suggesting delayed early neurogenesis. In agreement, BrdU birthdating studies, performed by BrdU labeling precursors at E13.5 and analyzing cell fate at E19.5, indicated that more E13.5 p57KO neurons occupied lower cortical layers (Fig. 6C-E) and expressed Tbr1 compared with wild type (Fig. 6F-H). Thus, early p57KO precursors remain in a proliferative state, delaying the normal timetable of neurogenesis.

By contrast, at E15.5, mutants exhibited an increased leaving fraction (Fig. 7A). Detailed bin analysis indicated a bi-modal distribution of postmitotic (BrdU$^+$/Ki67$^-$) cells (Fig. 7C,D). These two peaks of postmitotic cells were described previously as Q-slow and Q-rapid (Takahashi et al., 1996b; Goto et al., 2004). In mutants, the Q-rapid population was increased twofold (Fig. 7D), suggesting a mechanism for enhanced postmitotic neurogenesis. In agreement, Tbr1$^+$ layer 6 neurons in E16.5 mutants were increased by 19% (Fig. 7B) while Tbr1$^+$ subplate cells were unchanged (not shown). In aggregate, in the absence of p57^{KIP2}, early neurogenesis is delayed, probably favoring precursor pool expansion; later, neuron production is increased, which accounts for cortical expansion.

Effects of p57^{KIP2} deficiency on cortical cytoarchitecture

As p57KO embryos exhibited delayed early neurogenesis followed by excess neuron production, we explored cortical composition by measuring protein levels of Tbr1 and Cux1, markers of lower and upper layers, respectively. Tbr1 protein levels were increased twofold in p57^{KIP2} mutants, while Cux1 was unchanged (Fig. 8A), suggesting cortical layers are differentially affected. Thus, we assessed neuronal composition stereologically using layer-specific markers: Tbr1 (SP-layer 6), Ctip2 (layer 5) and Cux1 (layers 2-3). At E18.5, immunoreactive neurons for each marker were found in all layers, but were more densely packed and labeled in specific layers (Fig. 8B), as reported previously (Molyneaux et al., 2007), to which we restricted counting. Overall laminar organization was unaltered in mutant cortex though radial thickness of layer 6 plus SP (Tbr1) was modestly increased (Fig. 8B,C). More importantly, Tbr1$^+$ neurons were increased by 25%, Ctip2$^+$ neurons by 21% and Cux1$^+$ neurons by 13%, in p57KO embryos (Fig. 8D). Thus, neuron production was increased in each CP layer in p57KO cortex, with greatest effects on lower layers.

As the p57^{KIP2} gene is expressed in a high caudal low rostral gradient (Genepaint #ES628), we assessed potential regional variations by measuring the thickness of the CP and cortical layers at four rostrocaudal locations in the dorsomedial and lateral cortices (supplementary material Fig. S4A,B). The E18.5 mutants exhibited increases in total CP and layer 6 thickness in the dorsomedial cortex only, with greater effects caudally (supplementary material Fig. S4C), consistent with the gene expression pattern.

Postnatal p57KO mice exhibit increased lower layer neurons preferentially, whereas p27^{KIP1} mutants exhibit excess upper layer neurons

Although rare, some p57KO animals (n=4) survived until P10, as previously observed (Zhang et al., 1997). Thus, we (1) studied postnatal stages when cortical migration is complete, analyzed (2) interneurons and (3) glia, and (4) compared cytoarchitecture to p27^{KIP1} mutants, which overproduce upper layer neurons (Goto et al., 2004).

Postnatal p57^{KIP2} mutants appeared smaller than wild type, as reported previously (Zhang et al., 1997). Body (wild type, 6.3±0.34 g; p57KO, 5.1±0.94 g; n=4/group; mean±s.e.m.; P>0.05) and brain (wild type, 365.0±4.88 mg; p57KO, 336.3±12.53 mg; P>0.05) weights were non-significantly diminished. Mutant brains appeared normal, though the midbrain appeared larger (Fig. 9A).

We assessed cortical layer thickness, cell numbers and survival using immunohistochemistry. Radial thickness of layer 6 plus SP specifically was increased in mutants (Fig. 9B-D,J), similar to E18.5. Moreover, there was a 28% increase in cells expressing neuronal marker NeuN (Fig. 9B,E). By contrast, parvalbumin$^+$ interneurons and S100β$^+$ glia were markedly decreased in mutants, while CC1$^+$ oligodendrocytes were unchanged (Fig. 9K). Finally, cell death, assessed by activated caspase 3, was unchanged (wild type, 3.9±0.87; p57KO, 4.1±1.06; mean cells/section±s.e.m.; P>0.05). These results support prenatal observations indicating neuron overproduction in p57^{KIP2} mutants and suggest defects in glial cell and interneuron development.

Furthermore, we compared cortical cytoarchitecture of P10 p57KOs with p27^{KIP1} mutants. p57KO mice exhibited differential increases in laminar neurons, with greater effects in lower layers (+43% for Tbr1 versus +12% for Cux1; Fig. 9C-E). Although p27^{KIP1} mutants also displayed increased NeuN$^+$ neurons (Fig. 9F,I), increases were greater in superficial layers: 39% for Cux1 and no change in layer 6 (Fig. 9F-I). Thus, p57KO mice exhibit increased neurons preferentially in deep layers, whereas p27KOs overproduced superficial layers only, as reported previously (Goto et al., 2004).

p57^{KIP2} regulates both RGC and IPC proliferation whereas p27^{KIP1} controls only IPCs

As our studies of p57^{KIP2}- and p27^{KIP1}-deficient mice suggest CKIs differentially regulate laminar neurogenesis, we compared p57^{KIP2} and p27^{KIP1} developmental expression and regulation of apical and basal precursor proliferation.

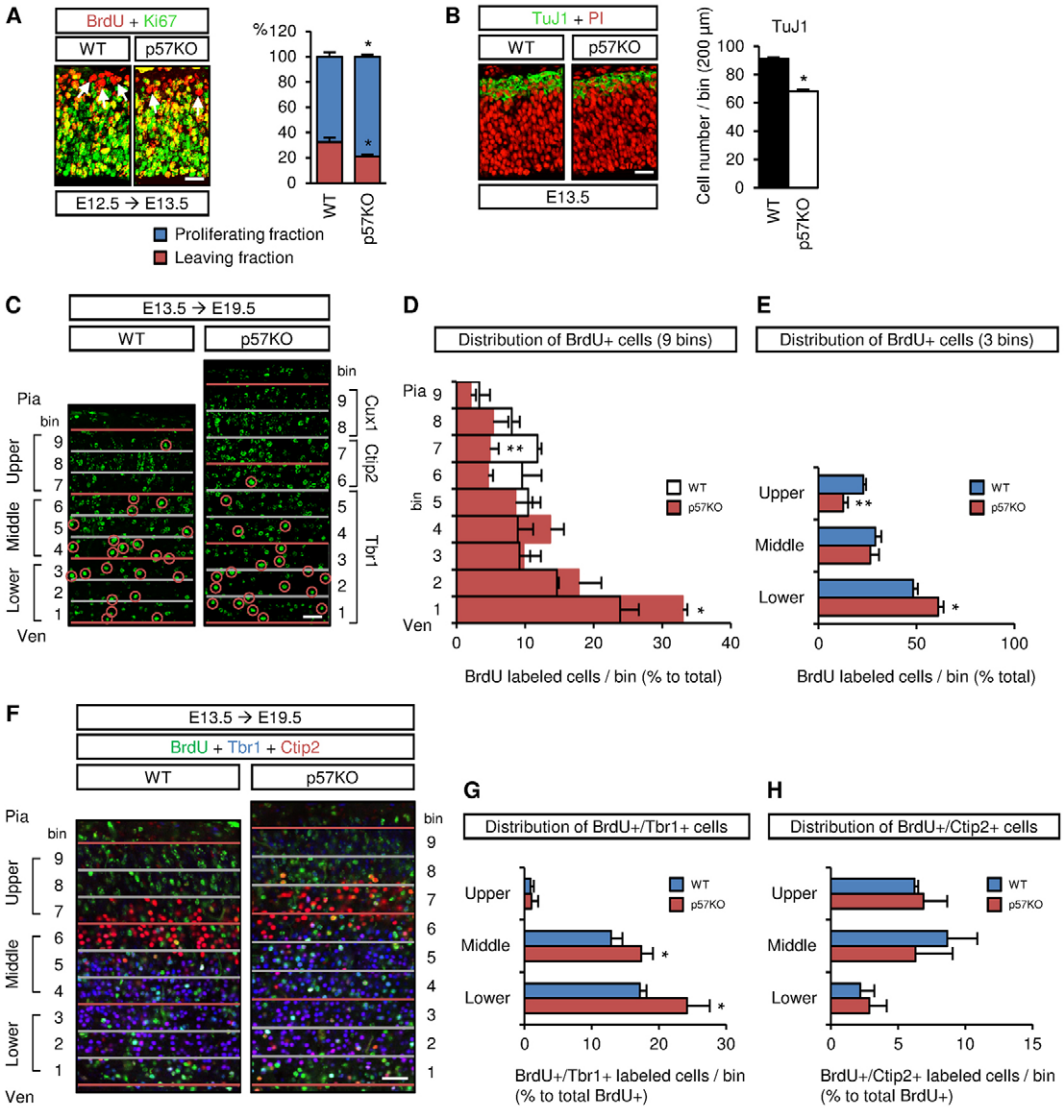

Fig. 6. Precursor cell cycle exit was decreased from E12.5 to E13.5 in p57KO cortex. (**A**) E13.5 frontal sections were double-labeled for Ki67 and BrdU following BrdU injection at E12.5. The proportion of cells leaving the cycle [BrdU$^+$/Ki67$^-$ (arrows) over total BrdU$^+$] was decreased in p57KO embryos (*n*=3 animals/group). (**B**) TuJ1$^+$ neurons were decreased in E13.5 mutants (*n*=3/group). (C-H) Birthdating analysis. Pregnant mice injected with BrdU on E13.5 were analyzed by immunohistochemistry at E19.5. (**C-E**) Distribution on E19.5 of neurons born on E13.5. (C) Frontal sections were divided into nine bins of equal height and fixed width, and cells exhibiting strong and homogeneous labeling were counted (D). (E) Bins 1-3, 4-6 and 7-9 were regrouped as lower, middle and upper bins. More p57KO cells born on E13.5 accumulate in the lower bin. (**F-H**) Cell fate of E13.5 born neurons. (F) E19.5 frontal sections were triple labeled for BrdU (green), Tbr1 (blue) and Ctip2 (red). (G) BrdU$^+$/Tbr1$^+$ and (H) BrdU$^+$/Ctip2$^+$ cells were counted in lower, middle and upper bins. More cells born on E13.5 in the p57KO differentiated into Tbr1$^+$ neurons in lower/middle bin than in wild type, whereas there was no statistical difference in Ctip2$^+$ upper neurons (*n*=4/group). Ven, ventricle. Data are mean±s.e.m. **P*<0.05, ***P*<0.01. Scale bars: 25 µm in A,B; 50 µm in C,F.

p27^{KIP1} protein expression, examined using a previously characterized antibody (Tury et al., 2011), localized to cell nuclei in proliferative and postmitotic compartments at E14.5 (Fig. 10B,E,H,K). While double immunolabeling indicated p27^{KIP1} expression overlapped with p57^{KIP2} in CP (Fig. 10A-F), there were divergent patterns in proliferative regions. In frontomedial (Fig. 10A-C) and dorsomedial (Fig. 10D-F) cortex, cells in the VZ expressed p57^{KIP2} alone, whereas virtually no cells expressed p27^{KIP1}. This was further supported by absence of p27^{KIP1} expression in Pax6$^+$ RGCs (Fig. 10G-I). In SVZ, p27^{KIP1} was weakly expressed in some Tbr2$^+$ IPCs, while expression appeared stronger in CP (Fig. 10J-L).

Apical and basal precursor proliferation was assessed in p27KOs at E14.5 (peak layer 4-5 neurogenesis) and E16.5 (peak layers 2-3) using mitotic marker PH3, as performed for p57KOs (Fig. 4A-D). Interestingly, at E14.5, only p57KOs exhibited increased mitoses in total, apical or basal precursors, suggesting earlier developmental function. Regardless of age, apical divisions were increased, although modestly, in only p57KOs, whereas basal divisions increased in both mutants (Fig. 11A,B). The basal division increase was greater in p57KO cortex at E14.5, during deep layer neurogenesis (+90% in p57KO versus 30% in p27KO; Fig. 4D, Fig. 11A-C). The relationship reversed at E16.5, during superficial layer neurogenesis, with greater basal division increases

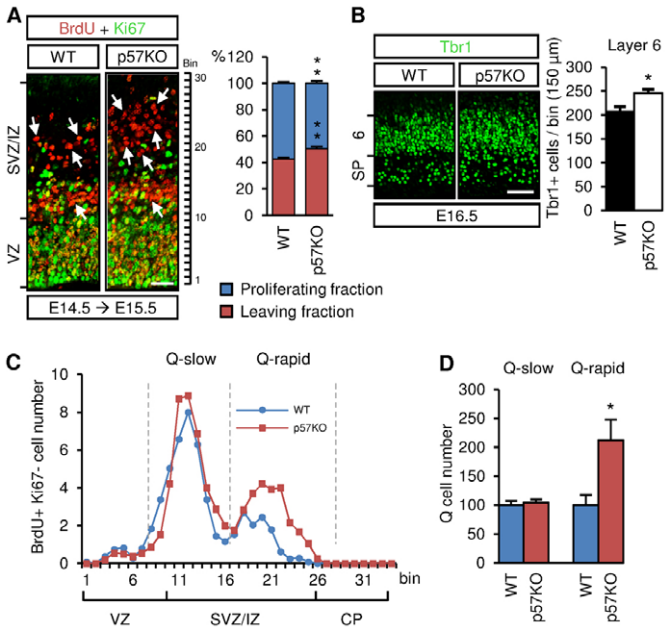

Fig. 7. Neuron production was increased during middle/late neurogenesis in p57KO cortex. (**A**) Cells leaving the cycle, defined by $BrdU^+/Ki67^-$ (arrows), were increased from E14.5 to E15.5 in $p57^{KIP2}$ mutants (n=4/group). (**B**) $Tbr1^+$ layer 6 neurons, distinguished from subplate (SP) based on cell densities and cell-free gap, were increased in mutants. (**C**) Radial distribution of precursors leaving the cycle from E14.5 to E15.5 revealed two peaks, one in lower SVZ (Q-slow) and the second in upper IZ (Q-rapid). (**D**) Q-rapid was increased twofold in mutant cortex. Data are mean±s.e.m. *P<0.05, **P<0.01. Scale bars: 50 µm in A; 100 µm in B.

in p27KO cortices (+114% in p27KO versus 42% in p57KO; Fig. 11B,D,E). Altogether, our observations suggest: (1) that $p57^{KIP2}$ regulates proliferation of both RGCs and IPCs while $p27^{KIP1}$ may act selectively on IPCs, in agreement with their distributions (Fig. 10); (2) that the two CKIs control layer-specific neurogenesis by regulating precursor proliferation at different developmental stages; and (3) that IPCs generate neurons for both lower and upper cortical layers.

DISCUSSION

Our observations suggest $p57^{KIP2}$ is a major regulator of precursor proliferation during embryonic cortical development. The CKI controls the size of precursor pools and consequently neuron production by regulating the rate of cell cycle progression during G1 and the balance of cell cycle re-entry to withdrawal. Interestingly, $p57^{KIP2}$ regulates both RGC and IPC cell cycle dynamics, while related $p27^{KIP1}$ controls IPCs only. Furthermore, the CKIs regulate proliferation at different stages of corticogenesis, differentially affecting cortical laminar neurogenesis.

$p57^{KIP2}$ is expressed in RGC and IPC precursors and postmitotic neurons

$p57^{KIP2}$ protein expression starts with the onset of corticogenesis, consistent with its mRNA (Tury et al., 2011). Spatially, $p57^{KIP2}$ was expressed in both RGCs and IPCs, consistent with its role as G1 regulator (Sherr and Roberts, 1999), as well as postmitotic neurons, a pattern suggesting $p57^{KIP2}$ expression starts during G1 phase of the final cycle in precursors undergoing cell cycle exit (G1→G0), and extends into the postmitotic state, consistent with studies in retina and midbrain (Dyer and Cepko, 2001; Ye et al., 2009).

$p57^{KIP2}$ regulates cortical size and RGC and IPC proliferation

During late corticogenesis, $p57^{KIP2}$-deficient brains exhibited cortical enlargement associated with increased volume, thickness and cell number, suggesting $p57^{KIP2}$ regulates proliferation. In p57KO, we found increased precursor S-phase entry and mitoses in VZ and SVZ, producing increased numbers of RGCs and IPCs. Interestingly, mitoses were increased more in SVZ than VZ, supporting the theory that basal precursor proliferation is tightly controlled by $p57^{KIP2}$. Although our data suggest that $p57^{KIP2}$ regulates the cell cycle dynamics of IPCs directly, we cannot exclude the possibility that RGC pool expansion contributes to their increase, as recently shown (Lange et al., 2009; Pilaz et al., 2009). Regardless of enhanced proliferation, RGC and IPC divisions declined progressively with development, indicating that $p57^{KIP2}$ is probably not the prime regulator terminating corticogenesis. Alternatively, loss of $p57^{KIP2}$ function may be compensated by INK4 family of CKIs (Zindy et al., 1997; Coskun and Luskin, 2001).

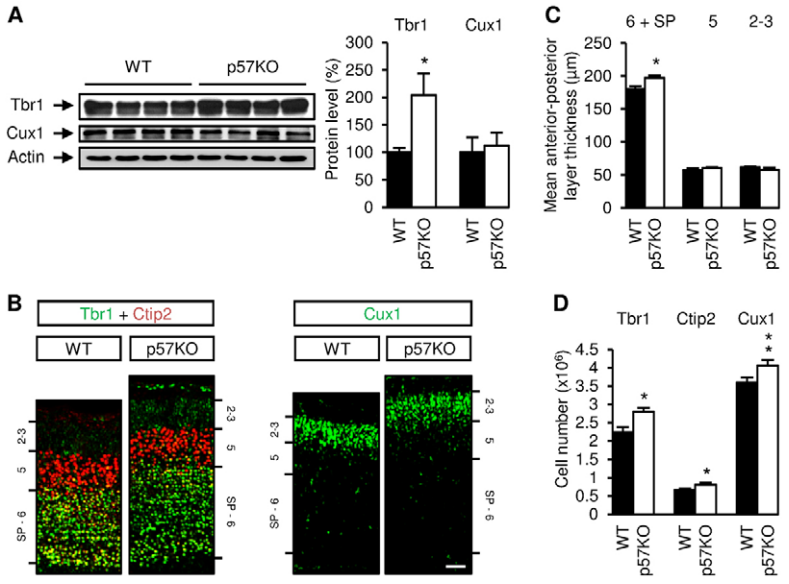

Fig. 8. p57KO embryos exhibited increased neuron production, preferentially in lower cortical layers. (**A**) Layer 6-SP marker Tbr1 protein level, assessed by western blot, was increased in E18.5 p57KO cortex, while layer 2-3 marker Cux1 was unchanged (n=4/group). (**B**) Immunolabeling of E18.5 frontal sections for Tbr1, Ctip2 and Cux1 in dorsomedial cortex. Layer 6 thickness appears larger in mutants. (**C**) Mean thickness of layer 6, measured over the anterior-posterior extent on sagittal sections, was modestly increased in p57KOs, while other layers were unaffected (n=3 animals/group, four sections/animal). (**D**) Total neurons in each layer, estimated by stereology, were increased in p57KO embryos (25.4% for Tbr1, 21.6% for Ctip2 and 13.0% for Cux1, n=4 animals/group). Data are mean±s.e.m. *P<0.05, **P<0.01, ***P<0.001. Scale bars: 100 µm.

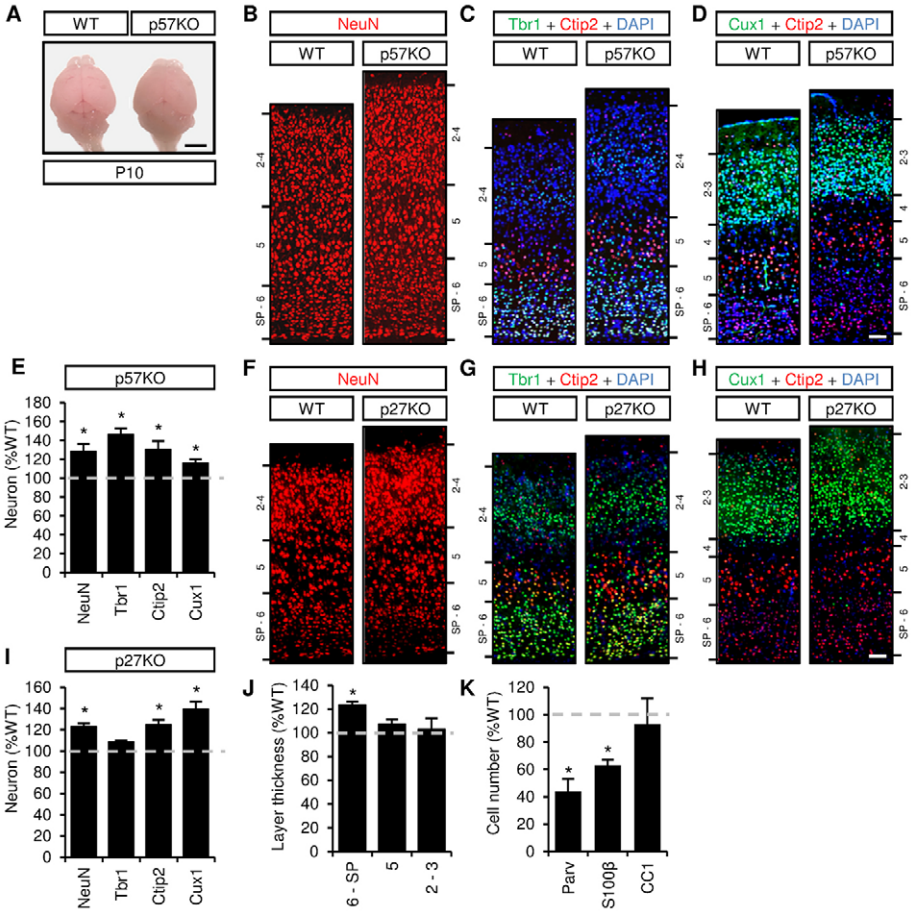

Fig. 9. Postnatal p57KO mice exhibited increased lower layer neurons preferentially while p27^{KIP1} mutants exhibited excess upper layer neurons. (**A**) Dorsal view of P10 wild-type and p57KO brains. (**B-K**) Frontal sections from P10 wild-type, p57KO and p27KO animals were immunolabeled for NeuN (B,F) or Ctip2 and Tbr1 (C,G) or Cux1 (D,H). Total neurons (NeuN$^+$) and neurons per layer were counted in dorsomedial cortex at mid-hemisphere in 100 μm bins. Neurons increased preferentially in (E) lower layers in p57KOs and (I) upper layers in p27KO mutants. (J) Layer 6 thickness was increased specifically in p57KOs. (K) Numbers of parvalbumin$^+$ interneurons (parv) and glia (S100β$^+$) were quantified on three non-consecutive sections/animal. Oligodendrocytes (CC1$^+$) were counted in 100 μm bins. Values represent percent control (n=4 animals/group). Data are mean±s.e.m. *P<0.05. Scale bars: 5 mm in A; 100 μm in B-D,F-H.

p57^{KIP2} regulates cell cycle length and the balance of cell cycle re-entry to withdrawal

Increased neuron numbers in p57KOs may be caused by: (1) an increased rate of precursor divisions producing population expansion; (2) a change in the balance of cell cycle re-entry to withdrawal; and/or (3) increased survival.

We found T_C was decreased in p57KO VZ precursors at E14.5 and E16.5, essentially owing to reduced T_{G1}. Experimental models suggest T_{G1} reduction promotes cell cycle re-entry at the expense of differentiation, and, conversely, lengthening T_{G1} induces cycle withdrawal and premature differentiation (Calegari et al., 2005; Lange et al., 2009; Pilaz et al., 2009). T_{G1} reduction in p57KO precursors was associated with increased precursor mitoses, and RGC and IPC numbers, supporting a link between T_C and size of precursor pools.

The change in cell cycle kinetics had profound effects on the balance between cell cycle re-entry and postmitotic cell production that were stage specific. At E13.5, the fraction of progenitors leaving the cycle as well as neuron production were decreased in p57KOs, suggesting precursors underwent additional proliferative divisions before cycle withdrawal, thereby expanding precursor pools. Conversely, at E15.5, the fractions of precursors leaving the cycle and producing neurons were increased, supporting the model that mutant precursors remain in cycle for a limited time and ultimately, withdraw to differentiate. Moreover, p57^{KIP2} expression in postmitotic neurons could suggest roles in maintaining quiescence, yet ectopic cell cycle re-entry of mutant cortical neurons was not observed. Furthermore, although loss of cycle control can initiate apoptosis (Cicero and Herrup, 2005), we detected no change in survival in p57KO cortex, a finding similar to p27KO (Goto et al., 2004).

p57^{KIP2} and p27^{KIP1} regulate distinct cortical layer neurogenesis by differentially controlling precursor populations at different stages

Our observations suggest p57^{KIP2} and p27^{KIP1} regulate proliferation of different cortical precursor populations, a conclusion also drawn in studies of retina (Dyer and Cepko, 2001). Spatial specialization has also been observed for positive G1 regulators, the D cyclins, during cortical development, with both cyclin D1 and D2 expressed in RGCs, whereas cyclin D2 alone is present in IPCs (Glickstein et al., 2009). These observations suggest that different mechanisms regulate proliferation/cell cycle exit of RGCs and IPCs, and that they rely on opposing activities of D cyclins and specific CIP/KIP family members, though inter-relationships remain unexplored.

The distribution of newly generated postmitotic cells in p57KO cortex was bimodal, one group leaving the VZ more rapidly (Q-rapid) than the other (Q-slow), similar to wild-type and p27KO mice (Goto et al., 2004). Although significance of these groups is unclear, they may represent differential mechanisms governing cell fate (Takahashi et al., 1996a; Goto et al., 2004). While absence of p57^{KIP2} or p27^{KIP1} had no influence on Q-slow cells, effects on Q-rapid cells were opposite, increased in p57KO cortex but diminished in p27KO (Goto et al., 2004), suggesting the CKIs regulate neurogenesis at different developmental stages.

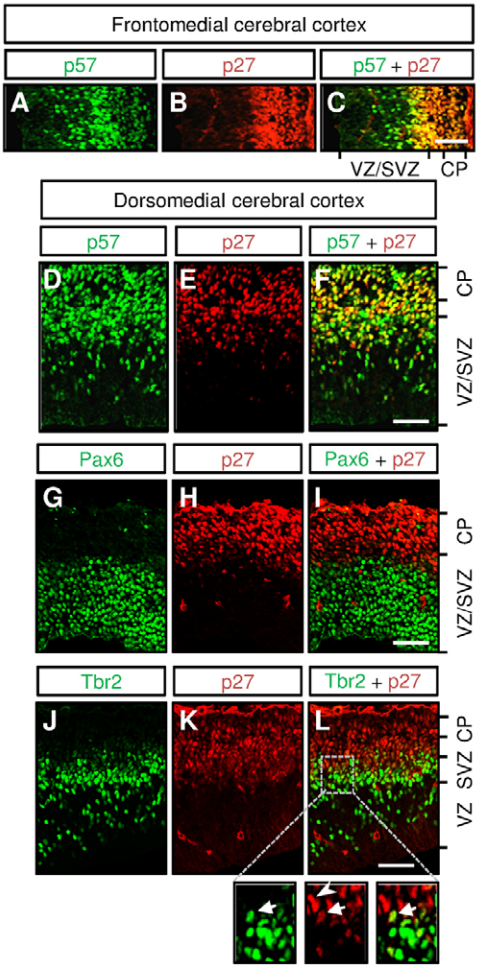

Fig. 10. p27KIP1 protein expression in E14.5 cortex. (**A-F**) In frontomedial and dorsomedial cortex, p27KIP1 and p57KIP2 were frequently co-expressed in CP, IZ and SVZ. By contrast, p57KIP2 but not p27KIP1 was expressed in proliferative VZ cells (see Fig. 2G,H). (**G-L**) p27KIP2 was virtually absent from Pax6+ RGCs, while it co-localized to some Tbr2+ IPCs (arrows, insets). Arrowhead in L indicates a p27KIP1+/Tbr2− cell. Scale bars: 100 μm.

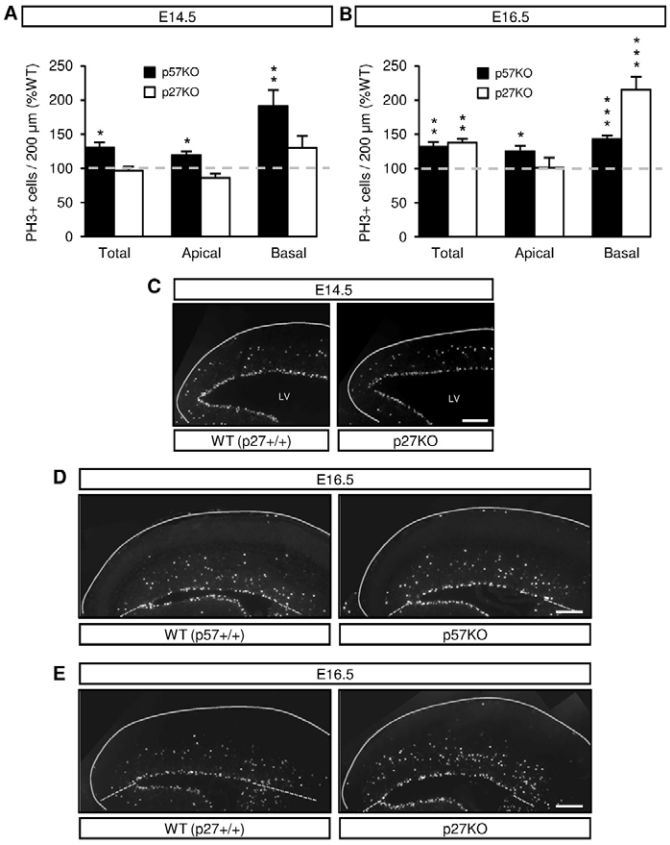

Fig. 11. p57KIP2 regulates both RGC and IPC proliferation whereas p27KIP1 controls only IPCs. (**A**,**B**) Total, apical and basal divisions (PH3+ cells)/area within 200 μm-wide bins in dorsomedial cortex were quantified on frontal, mid-hemisphere sections in (A) E14.5 and (B) E16.5 p57KO and p27KO embryos. Values represent percent control (*n*=4-6 embryos/genotype/age). Apical and basal mitoses increased at both ages in p57KO cortices, whereas only basal divisions increased in p27KO. Basal division increases were greater in p57KO cortex at E14.5 and in p27KO at E16.5. Data are mean±s.e.m. **P*<0.05, ***P*<0.01, ****P*<0.001. (**C-E**) PH3 immunolabeling of E14.5 and E16.5 wild-type, p57KO and p27KO embryos (compare Fig. 11C with Fig. 4D). Scale bars: 200 μm.

Although p57KIP2 deficiency did not alter the overall structure or inside-out sequence of laminar neurogenesis, mutant cortex exhibited increased thickness of layer 6 and excess neurons in all layers, with greatest effects in lower layers 5-6. The increased layer 6 neurogenesis probably resulted from increased cell cycle re-entry observed from E12.5 to E13.5 that was accompanied by a decrease in differentiating neurons, implying a delay in the normal timetable of neurogenesis. In agreement, more E13.5-born neurons expressed Tbr1 in lower layers in mutants, whereas more localized to upper layers in wild type. Furthermore, the increased proportion of Tbr1+ neurons was greater in dorsomedial than lateral cortex, and in caudal than rostral regions, supporting the notion that G1 regulators generate real differences in laminar cytoarchitecture (Dehay and Kennedy, 2007).

By contrast, p27KO mice displayed overproduction of neurons in layers 2-5 but not 6, as reported (Goto et al., 2004). Mitoses were increased in the SVZ but unchanged in RGC/VZ in p27KO, suggesting p27KIP1 regulates IPC proliferation specifically, consistent with its expression in Tbr2+ but not Pax6+ precursors. Exclusive expression of p27KIP1 in SVZ precursors may explain why previous studies detected no change in T_C within the p27KO VZ, while precursor cell cycle re-entry, probably defined in SVZ, was increased (Goto et al., 2004).

Furthermore, our data suggest distinct temporal regulation of IPC cell cycle dynamics: p57KIP2 plays a major role at E14.5, while p27KIP1 predominates at E16.5. In p27KOs, the selective increase in E16.5 IPC divisions supports their role in upper layer neurogenesis (Zimmer et al., 2004; Arnold et al., 2008). Conversely, p57KIP2 deficiency had a greater impact on IPCs than RGCs at E14.5, whereas neuron numbers mainly increased in layers 5-6. These results suggest IPCs also contribute to lower layer neurogenesis, an hypothesis supported by E13.5 birthdating analysis. However, further birthdating studies at later stages are required for definitive conclusions. These observations support a model whereby IPC progeny serve as transit-amplifying precursors producing projection neurons for all cortical layers (Haubensak et al., 2004; Sessa et al., 2008; Kowalczyk et al., 2009).

p57^{KIP2} may regulate interneuron and astrocyte production

An appropriate balance of projection neurons, interneurons and glial cells is crucial for brain function. At postnatal ages, in addition to increased projection neurons, p57^{KIP2} deficiency resulted in marked reduction of parvalbumin^{+} interneurons and astrocytes, whereas oligodendrocytes seemed unaffected.

As parvalbumin identifies mature interneurons, decreases in parvalbumin^{+} cells could be caused by either reduced GABAergic interneuron production and/or delayed parvalbumin expression. As p57^{KIP2} expression is observed as early as E12.5 in ganglionic eminences, the CKI may also regulate precursor proliferation in these regions (Ye et al., 2009).

Recently, we showed that p57^{KIP2} or p27^{KIP1} overexpression induced precursor cell cycle exit and precocious neuronal and astrocyte differentiation in vivo (Tury et al., 2011). While increased neurogenesis in p57^{KIP2} mutants results from prenatal precursor pool expansion, one might also expect increased gliogenesis, as observed in p27KOs (Goto et al., 2004). A limitation of the current p57KO is that postnatal development, when astrocytes are generated and interneurons integrate into cortical layers, is markedly compromised (Zhang et al., 1997), an issue that could be addressed by using conditional p57^{KIP2} inactivation models.

In conclusion, through differential spatiotemporal control of precursor proliferation, p57^{KIP2} and p27^{KIP1} regulate the size of cortical precursor pools and subsequent neurogenesis, thereby contributing in complementary fashion to the fine elaboration of radial and tangential cytoarchitecture of the developing cerebral cortex.

Acknowledgements

We thank Hussain Danish, Xiaofeng Zhou and Dr Olivier Camand for technical support and advice. We also thank Dr Mladen-Roko Rasin for providing reagents.

Funding

This work was supported by National Institutes of Health [NS32401]. Deposited in PMC for release after 12 months.

Competing interests statement

The authors declare no competing financial interests.

Supplementary material

Supplementary material available online at
http://dev.biologists.org/lookup/suppl/doi:10.1242/dev.067314/-/DC1

References

Alvarez-Bolado, G. and Swanson, L. W. (1996). Developmental brain maps: structure of the embryonic rat brain. Amsterdam: Elsevier.
Angevine, J. B., Jr and Sidman, R. L. (1961). Autoradiographic study of cell migration during histogenesis of cerebral cortex in the mouse. *Nature* **192**, 766-768.
Anthony, T. E., Klein, C., Fishell, G. and Heintz, N. (2004). Radial glia serve as neuronal progenitors in all regions of the central nervous system. *Neuron* **41**, 881-890.
Arnold, S. J., Huang, G. J., Cheung, A. F., Era, T., Nishikawa, S., Bikoff, E. K., Molnar, Z., Robertson, E. J. and Groszer, M. (2008). The T-box transcription factor Eomes/Tbr2 regulates neurogenesis in the cortical subventricular zone. *Genes Dev.* **22**, 2479-2484.
Bayer, S. A. and Altman, J. (1991). *Neocortical Development*. New York: Raven Press.
Berry, M., Rogers, A. W. and Eayrs, J. T. (1964). Pattern of cell migration during cortical histogenesis. *Nature* **203**, 591-593.
Calegari, F., Haubensak, W., Haffner, C. and Huttner, W. B. (2005). Selective lengthening of the cell cycle in the neurogenic subpopulation of neural progenitor cells during mouse brain development. *J. Neurosci.* **25**, 6533-6538.
Caviness, V. S., Bhide, P. G. and Nowakowski, R. S. (2008). Histogenetic processes leading to the laminated neocortex: migration is only a part of the story. *Dev. Neurosci.* **30**, 82-95.
Chenn, A. and Walsh, C. A. (2002). Regulation of cerebral cortical size by control of cell cycle exit in neural precursors. *Science* **297**, 365-369.
Cicero, S. and Herrup, K. (2005). Cyclin-dependent kinase 5 is essential for neuronal cell cycle arrest and differentiation. *J. Neurosci.* **25**, 9658-9668.
Coskun, V. and Luskin, M. B. (2001). The expression pattern of the cell cycle inhibitor p19(INK4d) by progenitor cells of the rat embryonic telencephalon and neonatal anterior subventricular zone. *J. Neurosci.* **21**, 3092-3103.
Cubelos, B., Sebastian-Serrano, A., Kim, S., Moreno-Ortiz, C., Redondo, J. M., Walsh, C. A. and Nieto, M. (2008). Cux-2 controls the proliferation of neuronal intermediate precursors of the cortical subventricular zone. *Cereb. Cortex* **18**, 1758-1770.
Dehay, C. and Kennedy, H. (2007). Cell-cycle control and cortical development. *Nat. Rev. Neurosci.* **8**, 438-450.
Delalle, I., Takahashi, T., Nowakowski, R. S., Tsai, L. H. and Caviness, V. S., Jr (1999). Cyclin E-p27 opposition and regulation of the G1 phase of the cell cycle in the murine neocortical PVE: a quantitative analysis of mRNA in situ hybridization. *Cereb. Cortex* **9**, 824-832.
Dyer, M. A. and Cepko, C. L. (2000). p57(Kip2) regulates progenitor cell proliferation and amacrine interneuron development in the mouse retina. *Development* **127**, 3593-3605.
Dyer, M. A. and Cepko, C. L. (2001). Regulating proliferation during retinal development. *Nat. Rev. Neurosci.* **2**, 333-342.
Englund, C., Fink, A., Lau, C., Pham, D., Daza, R. A., Bulfone, A., Kowalczyk, T. and Hevner, R. F. (2005). Pax6, Tbr2, and Tbr1 are expressed sequentially by radial glia, intermediate progenitor cells, and postmitotic neurons in developing neocortex. *J. Neurosci.* **25**, 247-251.
Fero, M. L., Rivkin, M., Tasch, M., Porter, P., Carow, C. E., Firpo, E., Polyak, K., Tsai, L. H., Broudy, V., Perlmutter, R. M. et al (1996). A syndrome of multiorgan hyperplasia with features of gigantism, tumorigenesis, and female sterility in p27(Kip1)-deficient mice. *Cell* **85**, 733-744.
Glickstein, S. B., Monaghan, J. A., Koeller, H. B., Jones, T. K. and Ross, M. E. (2009). Cyclin D2 is critical for intermediate progenitor cell proliferation in the embryonic cortex. *J. Neurosci.* **29**, 9614-9624.
Goto, T., Mitsuhashi, T. and Takahashi, T. (2004). Altered patterns of neuron production in the p27 knockout mouse. *Dev. Neurosci.* **26**, 208-217.
Gotz, M. and Barde, Y. A. (2005). Radial glial cells defined and major intermediates between embryonic stem cells and CNS neurons. *Neuron* **46**, 369-372.
Haubensak, W., Attardo, A., Denk, W. and Huttner, W. B. (2004). Neurons arise in the basal neuroepithelium of the early mammalian telencephalon: a major site of neurogenesis. *Proc. Natl. Acad. Sci. USA* **101**, 3196-3201.
Hayes, N. L. and Nowakowski, R. S. (2000). Exploiting the dynamics of S-phase tracers in developing brain: interkinetic nuclear migration for cells entering versus leaving the S-phase. *Dev. Neurosci.* **22**, 44-55.
Heins, N., Malatesta, P., Cecconi, F., Nakafuku, M., Tucker, K. L., Hack, M. A., Chapouton, P., Barde, Y. A. and Gotz, M. (2002). Glial cells generate neurons: the role of the transcription factor Pax6. *Nat. Neurosci.* **5**, 308-315.
Hicks, S. P. and D'Amato, C. J. (1968). Cell migrations to the isocortex in the rat. *Anat. Rec.* **160**, 619-634.
Itoh, Y., Masuyama, N., Nakayama, K., Nakayama, K. I. and Gotoh, Y. (2007). The cyclin-dependent kinase inhibitors p57 and p27 regulate neuronal migration in the developing mouse neocortex. *J. Biol. Chem.* **282**, 390-396.
Joseph, B., Wallen-Mackenzie, A., Benoit, G., Murata, T., Joodmardi, E., Okret, S. and Perlmann, T. (2003). p57(Kip2) cooperates with Nurr1 in developing dopamine cells. *Proc. Natl. Acad. Sci. USA* **100**, 15619-15624.
Kowalczyk, T., Pontious, A., Englund, C., Daza, R. A., Bedogni, F., Hodge, R., Attardo, A., Bell, C., Huttner, W. B. and Hevner, R. F. (2009). Intermediate neuronal progenitors (basal progenitors) produce pyramidal-projection neurons for all layers of cerebral cortex. *Cereb. Cortex* **19**, 2439-2450.
Lange, C., Huttner, W. B. and Calegari, F. (2009). Cdk4/cyclinD1 overexpression in neural stem cells shortens G1, delays neurogenesis, and promotes the generation and expansion of basal progenitors. *Cell Stem Cell* **5**, 320-331.
Mairet-Coello, G., Tury, A., Fellmann, D., Risold, P. Y. and Griffond, B. (2005). Ontogenesis of the sulfhydryl oxidase QSOX expression in rat brain. *J. Comp. Neurol.* **484**, 403-417.
Mairet-Coello, G., Tury, A. and DiCicco-Bloom, E. (2009). Insulin-like growth factor-1 promotes G(1)/S cell cycle progression through bidirectional regulation of cyclins and cyclin-dependent kinase inhibitors via the phosphatidylinositol 3-kinase/Akt pathway in developing rat cerebral cortex. *J. Neurosci.* **29**, 775-788.
Malatesta, P., Hack, M. A., Hartfuss, E., Kettenmann, H., Klinkert, W., Kirchhoff, F. and Gotz, M. (2003). Neuronal or glial progeny: regional differences in radial glia fate. *Neuron* **37**, 751-764.
Martynoga, B., Morrison, H., Price, D. J. and Mason, J. O. (2005). Foxg1 is required for specification of ventral telencephalon and region-specific regulation of dorsal telencephalic precursor proliferation and apoptosis. *Dev. Biol.* **283**, 113-127.
McConnell, S. K. (1988). Development and decision-making in the mammalian cerebral cortex. *Brain Res.* **472**, 1-23.

Miyata, T., Kawaguchi, A., Saito, K., Kawano, M., Muto, T. and Ogawa, M. (2004). Asymmetric production of surface-dividing and non-surface-dividing cortical progenitor cells. *Development* **131**, 3133-3145.
Molyneaux, B. J., Arlotta, P., Hirata, T., Hibi, M. and Macklis, J. D. (2005). Fezl is required for the birth and specification of corticospinal motor neurons. *Neuron* **47**, 817-831.
Molyneaux, B. J., Arlotta, P., Menezes, J. R. and Macklis, J. D. (2007). Neuronal subtype specification in the cerebral cortex. *Nat. Rev. Neurosci.* **8**, 427-437.
Nguyen, L., Besson, A., Heng, J. I., Schuurmans, C., Teboul, L., Parras, C., Philpott, A., Roberts, J. M. and Guillemot, F. (2006). p27kip1 independently promotes neuronal differentiation and migration in the cerebral cortex. *Genes Dev.* **20**, 1511-1524.
Noctor, S. C., Martinez-Cerdeno, V., Ivic, L. and Kriegstein, A. R. (2004). Cortical neurons arise in symmetric and asymmetric division zones and migrate through specific phases. *Nat. Neurosci.* **7**, 136-144.
Pilaz, L. J., Patti, D., Marcy, G., Ollier, E., Pfister, S., Douglas, R. J., Betizeau, M., Gautier, E., Cortay, V., Doerflinger, N. et al (2009). Forced G1-phase reduction alters mode of division, neuron number, and laminar phenotype in the cerebral cortex. *Proc. Natl. Acad. Sci. USA* **106**, 21924-21929.
Polleux, F., Dehay, C. and Kennedy, H. (1997). The timetable of laminar neurogenesis contributes to the specification of cortical areas in mouse isocortex. *J. Comp. Neurol.* **385**, 95-116.
Quinn, J. C., Molinek, M., Martynoga, B. S., Zaki, P. A., Faedo, A., Bulfone, A., Hevner, R. F., West, J. D. and Price, D. J. (2007). Pax6 controls cerebral cortical cell number by regulating exit from the cell cycle and specifies cortical cell identity by a cell autonomous mechanism. *Dev. Biol.* **302**, 50-65.
Rakic, P. (1988). Specification of cerebral cortical areas. *Science* **241**, 170-176.
Sessa, A., Mao, C.-A., Hadjantonakis, A.-K., Klein, W. H. and Broccoli, V. (2008). Tbr2 directs conversion of radial glia into basal precursors and guides neuronal amplification by indirect neurogenesis in the developing neocortex. *Neuron* **60**, 56-69.
Sherr, C. J. and Roberts, J. M. (1999). CDK inhibitors: positive and negative regulators of G1-phase progression. *Genes Dev.* **13**, 1501-1512.
Suter, B., Nowakowski, R. S., Bhide, P. G. and Caviness, V. S. (2007). Navigating neocortical neurogenesis and neuronal specification: a positional information system encoded by neurogenetic gradients. *J. Neurosci.* **27**, 10777-10784.
Takahashi, T., Nowakowski, R. S. and Caviness, V. S., Jr (1993). Cell cycle parameters and patterns of nuclear movement in the neocortical proliferative zone of the fetal mouse. *J. Neurosci.* **13**, 820-833.
Takahashi, T., Nowakowski, R. S. and Caviness, V. S., Jr (1995a). The cell cycle of the pseudostratified ventricular epithelium of the embryonic murine cerebral wall. *J. Neurosci.* **15**, 6046-6057.
Takahashi, T., Nowakowski, R. S. and Caviness, V. S., Jr (1995b). Early ontogeny of the secondary proliferative population of the embryonic murine cerebral wall. *J. Neurosci.* **15**, 6058-6068.
Takahashi, T., Nowakowski, R. S. and Caviness, V. S., Jr (1996a). Interkinetic and migratory behavior of a cohort of neocortical neurons arising in the early embryonic murine cerebral wall. *J. Neurosci.* **16**, 5762-5776.
Takahashi, T., Nowakowski, R. S. and Caviness, V. S., Jr (1996b). The leaving or Q fraction of the murine cerebral proliferative epithelium: a general model of neocortical neuronogenesis. *J. Neurosci.* **16**, 6183-6196.
Tang, X., Falls, D. L., Li, X., Lane, T. and Luskin, M. B. (2007). Antigen-retrieval procedure for bromodeoxyuridine immunolabeling with concurrent labeling of nuclear DNA and antigens damaged by HCl pretreatment. *J. Neurosci.* **27**, 5837-5844.
Tarabykin, V., Stoykova, A., Usman, N. and Gruss, P. (2001). Cortical upper layer neurons derive from the subventricular zone as indicated by Svet1 gene expression. *Development* **128**, 1983-1993.
Tarui, T., Takahashi, T., Nowakowski, R. S., Hayes, N. L., Bhide, P. G. and Caviness, V. S. (2005). Overexpression of p27 Kip 1, probability of cell cycle exit, and laminar destination of neocortical neurons. *Cereb. Cortex* **15**, 1343-1355.
Tury, A., Mairet-Coello, G. and Dicicco-Bloom, E. (2011). The cyclin-dependent kinase inhibitor p57Kip2 regulates cell cycle exit, differentiation, and migration of embryonic cerebral cortical precursors. *Cereb. Cortex* **21**, 1840-1856.
Vaccarino, F. M., Schwartz, M. L., Raballo, R., Nilsen, J., Rhee, J., Zhou, M., Doetschman, T., Coffin, J. D., Wyland, J. J. and Hung, Y. T. (1999). Changes in cerebral cortex size are governed by fibroblast growth factor during embryogenesis. *Nat. Neurosci.* **2**, 246-253.
Ye, W., Mairet-Coello, G., Pasoreck, E. and Dicicco-Bloom, E. (2009). Patterns of p57Kip2 expression in embryonic rat brain suggest roles in progenitor cell cycle exit and neuronal differentiation. *Dev. Neurobiol.* **69**, 1-21.
Zhang, P., Liegeois, N. J., Wong, C., Finegold, M., Hou, H., Thompson, J. C., Silverman, A., Harper, J. W., DePinho, R. A. and Elledge, S. J. (1997). Altered cell differentiation and proliferation in mice lacking p57KIP2 indicates a role in Beckwith-Wiedemann syndrome. *Nature* **387**, 151-158.
Zimmer, C., Tiveron, M. C., Bodmer, R. and Cremer, H. (2004). Dynamics of Cux2 expression suggests that an early pool of SVZ precursors is fated to become upper cortical layer neurons. *Cereb. Cortex* **14**, 1408-1420.
Zindy, F., Soares, H., Herzog, K. H., Morgan, J., Sherr, C. J. and Roussel, M. F. (1997). Expression of INK4 inhibitors of cyclin D-dependent kinases during mouse brain development. *Cell Growth Differ.* **8**, 1139-1150.